Atmospheric Research 298 (2024) 107143

Contents lists available at ScienceDirect

Atmospheric Research

journal homepage: www.elsevier.com/locate/atmosres

Terrain effects of the Tibetan Plateau on dust aerosol distribution over the Tarim Basin, China

Chenglong Zhou [a,b,c,1], Xinghua Yang [a,d,1], Yuzhi Liu [b,c,*], Qingzhe Zhu [h], Yongkun Xie [b,c], Fan Yang [a,e,f,g], Mamtimn Ali [a,e,f,g], Wen Huo [a,e,f,g], Qing He [a,e,f,g], Lu Meng [a,e,f,g]

[a] Institute of Desert Meteorology, China Meteorological Administration, Urumqi 830002, China
[b] Key Laboratory for Semi-Arid Climate Change of the Ministry of Education, College of Atmospheric Sciences, Lanzhou University, Lanzhou 730000, China
[c] Collaborative Innovation Center for Western Ecological Safety, Lanzhou University, Lanzhou 730000, China
[d] College of Geographical Sciences, Shanxi Normal University, Taiyuan 030000, China
[e] Taklimakan National Station of Observation and Research for Desert Meteorology in Xinjiang, Urumqi 830002, China
[f] Taklimakan Desert Meteorology Field Experiment Station, China Meteorological Administration, Urumqi 830002, China
[g] Xinjiang Key Laboratory of Desert Meteorology and Sandstorm, Urumqi 830002, China
[h] College of Oceanic and Atmospheric Sciences, Ocean University of China, Qingdao 266100, China

ARTICLE INFO

Keywords:
Dust aerosol distribution
Meteorological field
Plateau altitude
Tarim Basin

ABSTRACT

Dust events are frequent in the Tarim Basin because of its underlying desert surface; moreover, meteorological conditions under the influence of the surrounding high terrains, especially the Tibetan Plateau, may also trigger dust events. However, the terrain effect of the Tibetan Plateau on the dust aerosol distribution over the Tarim Basin remains unclear. This study aimed to investigate the impact of the Tibetan Plateau terrain on the dust aerosol variations in three dust events over the Tarim Basin using the Weather Research and Forecasting Chemistry model. With decreasing altitude of the Tibetan Plateau, dust concentration (DC) decreased in the upper layers and increased in the low layers. The DC within the entire atmospheric layers increased by 8.52%, 24.03%, and 43.05% on average during three dust events at Tibetan Plateau altitudes of 3000 m, 2000 m, and 1000 m, respectively, thereby indicating that the DC in the lower layers increasingly dominated the entire atmospheric layers as the Tibetan Plateau altitude decreased. Low-elevation terrain enhanced the planetary boundary layer height, near-surface wind speed, and surface air temperature, but weakened atmospheric stratification stability, all of which are beneficial for strengthening dust emissions and vertical mixing in the lower layers of the Tarim Basin. Furthermore, a decrease in the Tibetan Plateau altitude led to forming a vertical circulation, with the south to rise and the north to sink over the Tarim Basin. Meteorological field and vertical circulation could adequately explain the changes in the distribution of dust aerosols over the Tarim Basin. Overall, this study enhances our understanding of the effect of the Tibetan Plateau terrain on changes in the dust aerosol in the Tarim Basin and surrounding central Asian regions.

1. Introduction

Dust aerosols are important driving factors of global climate change and are equivalent to greenhouse gases, land use activities, and solar activity (Liu et al., 2014; Jia et al., 2018; Liu et al., 2020; Shao et al., 2022; Luo et al., 2022). The inhomogeneous distribution of dust aerosols can redistribute solar radiation vertically, thereby changing the dynamic and thermal structures of the atmosphere (Zhou et al., 2022a, 2022b). Furthermore, dust aerosols directly affect the balance of the Earth's radiation budget by absorbing and scattering solar radiation, that is, aerosol-radiation interaction, and they also alter cloud microphysical properties, including aerosol-cloud interaction, to indirectly influence precipitation (Huang et al., 2009, 2014; Sakaeda et al., 2011; Zhang et al., 2015; Liu et al., 2011, 2013). Dust aerosols also considerably impact the marine biochemical cycle, atmospheric environment, human health, and agricultural production (Mahowald, 2011; Prospero et al.,

* Corresponding author at: Key Laboratory for Semi-Arid Climate Change of the Ministry of Education, College of Atmospheric Sciences, Lanzhou University, Lanzhou 730000, China.
E-mail address: liuyzh@lzu.edu.cn (Y. Liu).
[1] C. Zhou and X. Yang: these authors contributed equally to this work.

https://doi.org/10.1016/j.atmosres.2023.107143
Received 3 September 2023; Received in revised form 2 November 2023; Accepted 26 November 2023
Available online 5 December 2023

2014; Hoffmann and Funk, 2015). Therefore, understanding the distribution of dust aerosols is crucial.

Tarim Basin is a key source area of dust aerosols in China and East Asia, with annual total dust aerosol emissions accounting for approximately 35.0% of those in East Asia (Liu et al., 2016b; Chen et al., 2017). In China, the highest occurrence of floating dust weather is observed the Tarim Basin (Wang et al., 2003), especially in the south of the basin, accounting for more than 60% of the total dust days (Zhou et al., 2020). In this basin, a single floating dust event generally lasts for more than 7–10 d, and the historical extreme for the longest duration has been reported to be up to 64 d (Meng et al., 2022). Overall, the high frequency and long duration of floating dust in the Tarim Basin are extremely rare in arid and semi-arid regions worldwide (Yang et al., 2016; Chen et al., 2020). Therefore, Tarim Basin serves as a natural testing ground for studying dust structures in the region.

Neutral or unstable atmospheric stratification is not conducive to the sedimentation of dust particles, which maintains dust events (Chamecki et al., 2007; Pan et al., 2013). The input of exogenous sand dust and the stable boundary layer structure are the main reasons for maintaining floating dust weather (Li et al., 2020; Zhou et al., 2022b). Further, inversion and calm winds do not facilitate the diffusion of pollutants in the vertical and horizontal directions, which can lead to pollutant accumulation in urban areas, forming continuous floating dust weather (Zhang and Li, 2014; Li et al., 2021). Although many studies have investigated the impact on the dust aerosol distribution, the influence of terrain on the aerosol distribution is still limited.

Tarim Basin is to the north of the Tibetan Plateau. To date, the effect of the Tibetan Plateau terrain on the dust structure in the Tarim Basin remains unclear. Therefore, in this study, the impact of the Tibetan Plateau terrain on the dust distribution over the Tarim Basin was assessed based on the Weather Research and Forecasting coupled with a chemistry (WRF-Chem) model combined with reanalysis data.

The remaining manuscript is organized as follows: Section 2 describes the model and experimental setup. Section 3 presents the evaluation results of the simulated surface air temperature (SAT), wind speed at a height of 10 m (Wind_10), and aerosol optical thickness (AOD) data, along with the changes in the dust concentration (DC), Wind_10, SAT, planetary boundary layer (PBL) height, atmospheric stratification stability, and circulation field caused by the Tibetan Plateau terrain decreased. In Section 4, the impact of the Tibetan Plateau terrain on regional weather and climate has been discussed, and a mechanism diagram of the impact of the Tibetan Plateau terrain on the dust distribution over the Tarim Basin is provided. The main conclusions are presented in Section 5.

2. Data and methods

2.1. Reanalysis data

The Modern-Era Retrospective Analysis for Research and Applications Version 2 (MERRA-2) reanalysis dataset, provided by the National Aeronautics and Space Administration, was used in this study. The MERRA-2 dataset is a long-term atmospheric reanalysis dataset, which assimilates satellite observation data of aerosols and represents their interactions with other physical processes in the climate system (Molod et al., 2015; Gelaro et al., 2017). This dataset provided SAT, Wind_10, and AOD data with a 0.625° × 0.5° latitude/longitude spatial resolution and 72 pressure levels in the vertical direction to assess the WRF-Chem model.

2.2. Selected dust cases

In order to better illustrate the impact of the Tibetan Plateau terrain on the dust aerosol distribution over the Tarim Basin, the typical cases we choose follow these principles: firstly, the dust event process should last for a sufficient amount of time, and the duration of different dust cases was similar. Secondly, dust events were selected from a continuous period to ensure that they exhibit a similar environmental background for average processing. Spring was the frequent season of dust events in Tarim Basin (Zhou et al., 2020; Meng et al., 2022). The daily AOD data in the Tarim Basin were calculated from March to April 2020 using the MERRA-2 dataset, and three dust cases, namely, were selected according to the large AOD values: March 8–15 (Case 1), March 21–27 (Case 2), and April 10–18 (Case 3). The weather systems that affect these three dust cases were similar, but there were certain differences in their intensities.

2.3. WRF-Chem model

The WRF-Chem model version 3.8 version was used to investigate the effect of the Tibetan Plateau terrain on the dust distribution over the Tarim Basin. WRF-Chem is an atmospheric chemistry model developed by the National Center for Atmospheric Research, National Center for Environmental Prediction, and National Oceanic and Atmospheric Administration. It includes physical processes and chemical mechanisms related to aerosols (Grell et al., 2005). The Goddard Global Ozone Chemistry Aerosol Radiation and Transport scheme, which can simulate dust emission, deposition, and transport characteristics well (Ginoux et al., 2001, 2004; Huneeus et al., 2011; Liu et al., 2016a), was used as the dust emission scheme in the WRF-Chem model. Online coupling of meteorological and chemical fields is one of the advantages of WRF-Chem because it can reflect the interaction between meteorological elements and chemical processes. Therefore, the atmospheric environment can be simulated more accurately (Fast et al., 2006).

2.4. Experiment setup

Two nested domains, as shown in Fig. 1, were defined in the simulation, in which the red rectangle indicates the inner nested grid area. The horizontal resolutions of the outer and inner domains were 35 km × 35 km and 7 km × 7 km, respectively, and the temporal resolution of simulations was 1 h. The inner domain (red rectangle in Fig. 1) encompasses the Tibetan Plateau and Tarim Basin, which is the main study area. Vertically, 48 sigma layers were applied from the surface to a pressure of 50 hPa. In the control experiment (C_Exp), the original Tibetan Plateau terrain was used. The three sensitivity experiments (S_Exp) set the Tibetan Plateau terrain altitude to 1000 m (TP_1000), 2000 m (TP_2000), and 3000 m (TP_3000) respectively. Based on the three selected dust processes, the simulations were conducted for the time scales of March 6–15, March 19–27, and April 8–18, 2020. One set of C_Exp and three sets of S_Exp mentioned above were conducted for each dust process, such that 12 simulations were performed in this study. The simulation results of three dust processes from the same terrain experiment were averaged. Moreover, the impact of the Tibetan Plateau terrain on dust aerosol distribution over the Tarim Basin dust was evaluated by comparing the meteorological characteristics and dust aerosol concentrations between C_Exp and different S_Exps. The 6 h final analysis data with a spatial resolution of 1° × 1° and acquired from the National Center for Environmental Prediction were used for the initial and boundary conditions during the simulated period. The first two days of the simulations were discarded as the “spin-up” period to reduce the impact of initial conditions. The detailed physical and chemical schemes used in this model are listed in Table 1.

3. Results and analyses

3.1. Simulation and comparison with observations

Fig. 2 shows the SAT, Wind_10, and AOD simulated using the WRF-Chem model for the three dust cases selected in this study. The observational data were derived from MERRA-2. As shown in Fig. a1 and a2, the spatial distributions of SAT from MERRA-2 and WRF-Chem showed a

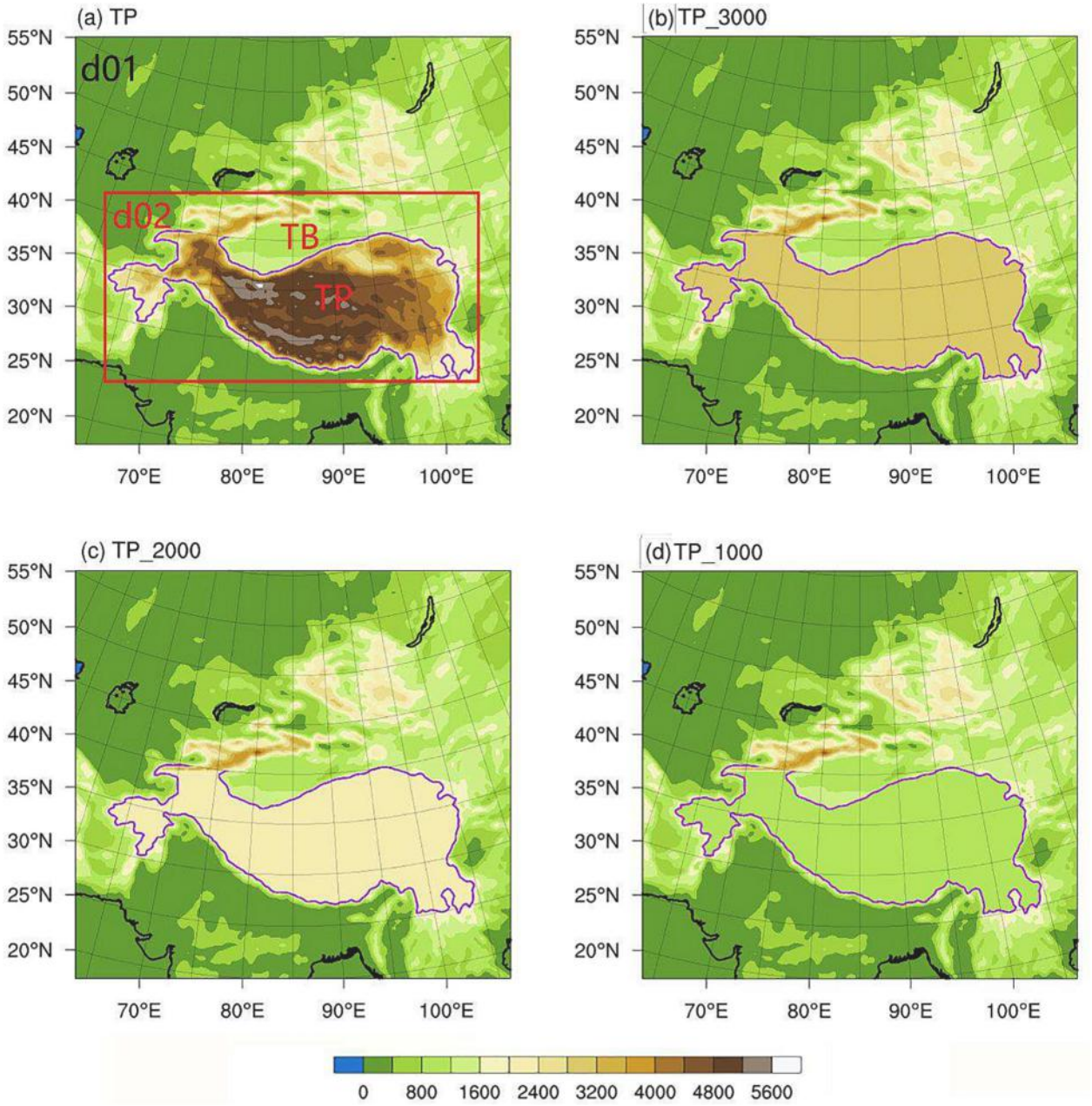

Fig. 1. (a) Modeling domains and terrain height (unit: m) over the vicinity of the Tarim Basin and Tibetan Plateau. The red rectangle indicates the inner nested area (d02). (b), (c), and (d) are the Tibetan Plateau terrains used in the S_Exp with an altitude of 1000 m (TP_1000), 2000 m (TP_2000), and 3000 m (TP_3000), respectively. The purple solid line in the figure is the isoline at an altitude of 2000 m, and the interior is the main area of the Tibetan Plateau and Tarim Basin. (For interpretation of the references to colour in this figure legend, the reader is referred to the web version of this article.)

Table 1
Model configuration used in the WRF-Chem simulations.

Processes	Schemes
Microphysics	Morrison two-moment
Cumulus convection	Kain–Fritsch
Planetary boundary	Yonsei University
Land surface	Noah land surface model
Longwave and shortwave radiation	RRTMG (Rapid Radiative Transfer Model for GCMs)
Gas-phase chemistry	RACM (Regional Atmospheric Chemistry Modeling) scheme
Aerosol chemistry	GOCART (Goddard Global Ozone Chemistry Aerosol Radiation and Transport)

high level of consistency, not only in pattern but also in intensity, especially in the Taklimakan Desert (TD). Although the reanalysis data and model simulation were correlated, the model slightly overestimated SAT in the east of the Tarim Basin. Furthermore, a comparison of Wind_10 and AOD between the results of MERRA-2 and WRF-Chem is shown in Fig. b1–b2 and c1–c2. Similar to SAT, the WRF-Chem model simulated Wind_10 and AOD in the Tarim Basin effectively. Compared to the reanalysis data, there were some marginal differences in the model simulations. Wind_10 was underestimated in the west of the Tarim Basin (mainly in the TD) and overestimated in the east of the Tarim Basin, while the model underestimated AOD in the TD.

The comparison indicated that although the reanalysis data and the model simulation results differed, the overall spatial distribution and intensity were consistent. Therefore, the model used in this study could

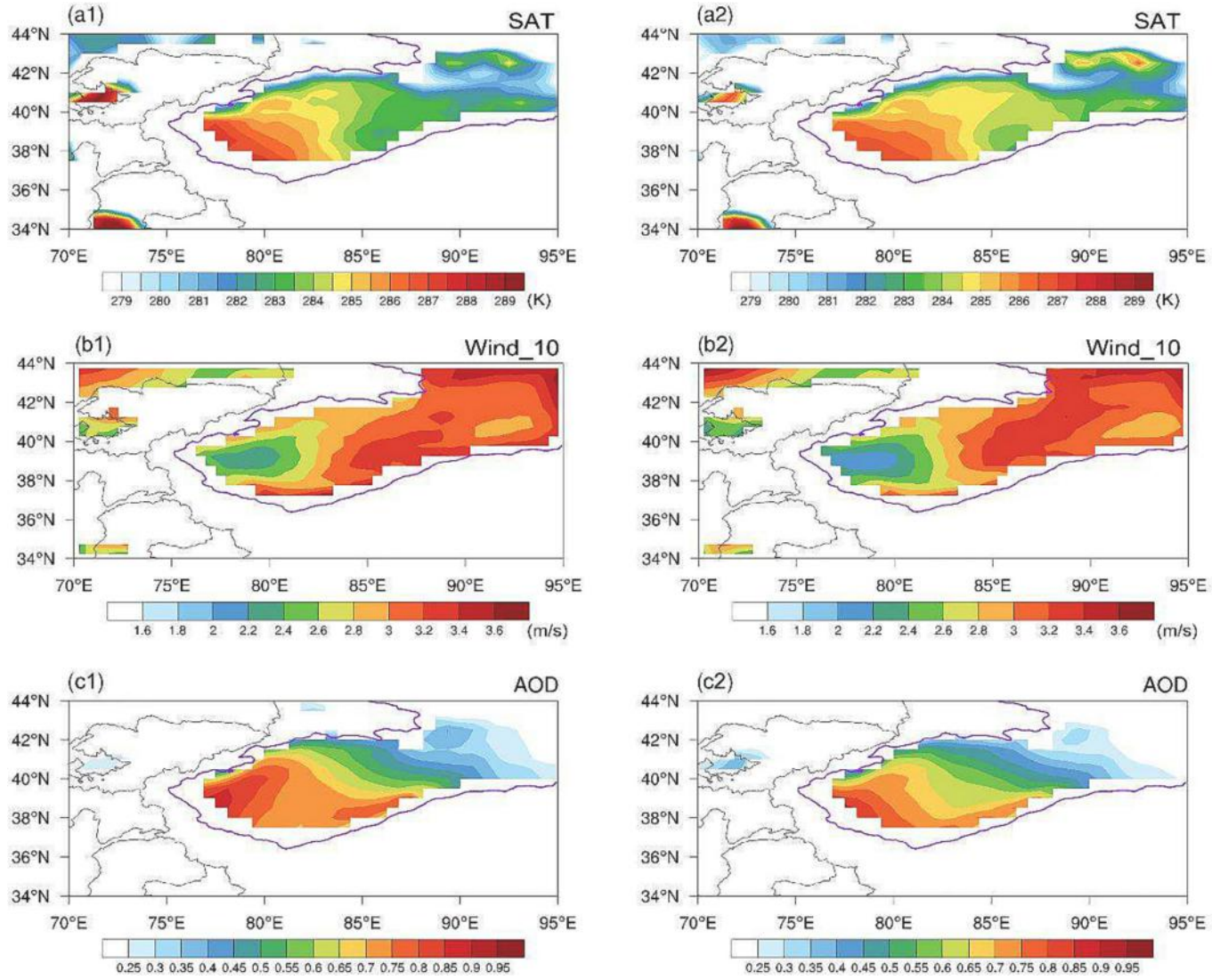

Fig. 2. Spatial distributions of SAT (a1), Wind_10 (b1), and AOD (c1) averaged during three dust cases obtained from MERRA-2. (a2), (b2), and (c2) are same as (a1), (b1), and (c1), respectively, but were obtained from the simulations. The purple rectangle indicates the Tarim Basin. (For interpretation of the references to colour in this figure legend, the reader is referred to the web version of this article.)

evaluate the DC, Wind_10, and SAT, among other variables.

3.2. *Effect of the Tibetan Plateau terrain on the dust distribution over the Tarim Basin*

Fig. 3a shows the vertical distribution of the DC under S_Exp and C_Exp conditions. In the three cases studies, as the Tibetan Plateau altitude decreased, characterization of the DC over the Tarim Basin decreased by upper layers and increased by low layers. Below 700 hPa, the enhancement of DC became more significant as the Tibetan Plateau altitude continuously decreased. However, this regular pattern was not observed in the upper layers. Therefore, the Tibetan Plateau altitude exhibited a significant impact on the dust aerosol distribution over the Tarim Basin, especially in the lower layers (Fig. 3a).

To more effectively investigate the influence of Tibetan Plateau terrain on the dust aerosol distribution over the Tarim Basin, we quantitatively calculated the DC changes at different levels of the Tarim Basin with decreasing altitude. Considering 700 hPa as the boundary line, the average DC increased by 13.72%, 31.39%, and 52.73% at altitudes below 700 hPa over the Tarim Basin as the Tibetan Plateau altitude decreased to 3000 m, 2000 m, and 1000 m, respectively. Particularly, DC increased by 20.93%, 47.32%, and 81.41% at 900 hPa as the Tibetan Plateau altitude decreased to 3000 m, 2000 m, and 1000 m, respectively (Fig. 3b). Contrastingly, for the upper levels (above 700 hPa), the average DC decreased by nearly 30% over the Tarim Basin as the Tibetan Plateau altitude decreased. From the perspective of the entire atmospheric layers, the average DC increased by 8.52%, 24.03%, and 43.05% in the Tarim Basin as the Tibetan Plateau altitude decreased to 3000 m, 2000 m, and 1000 m, respectively. This is was because the DC in the upper layers was significantly lower than that in the lower layers (Fig. 3a), and the reduction in the upper layers was far from sufficient to offset the increase in the lower layers. Therefore, the DC in the lower layers increasingly dominated the entire atmospheric layers as the Tibetan Plateau altitude decreased.

3.3. *Mechanism of the terrain effects of the Tibetan Plateau on dust distribution over the Tarim Basin*

To determine the reason for the different impacts of the Tibetan Plateau terrain on the dust aerosol distribution over the Tarim Basin, the reasons for alteration in the PBL height, Wind_10, SAT, atmospheric stratification stability, and circulation field according to the Tibetan

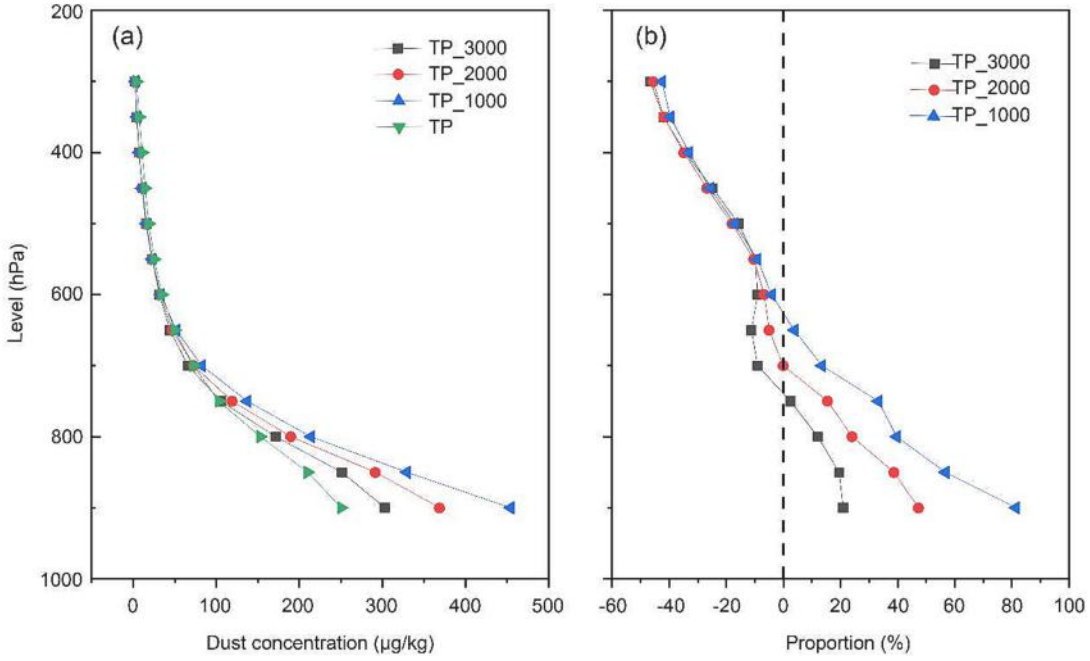

Fig. 3. Vertical distribution of dust aerosol concentration at different Tibetan Plateau altitudes (a) and the difference in the dust aerosol concentration between S_Exp and C_Exp (b), for the three dust cases, where the Tibetan Plateau altitudes were set to 3000 m (black line), 2000 m (red line), and 1000 m (blue line), respectively. (For interpretation of the references to colour in this figure legend, the reader is referred to the web version of this article.)

Plateau terrain were further investigated.

The PBL directly affected the spatiotemporal distribution of dust. Turbulent motion is the dominant form of atmospheric motion in the PBL (Garratt, 1994), where dust mainly accumulates. Therefore, we analyzed the effect of the Tibetan Plateau terrain on the PBL of the Tarim Basin. Fig. 4 shows the mean PBL heights at different Tibetan Plateau altitudes. The mean PBL height was 907.26–1319.08 m during the three dust cases, indicating that PBL height decreased significantly with the occurrence of dust event. The result was consistent with the findings of Zhou et al. (2022b). The PBL height increased slightly as the Tibetan Plateau altitude decreased. The mean PBL height was 923.63–1331.44 m, 918.87–1373.24 m, and 924.07–1386.32 m as the Tibetan Plateau altitude decreased to 3000 m, 2000 m and 1000 m, respectively. The increase in PBL height demonstrated that the decrease in the Tibetan Plateau altitude was beneficial for the diffusion and transportation of dust in the lower layers of the Tarim Basin.

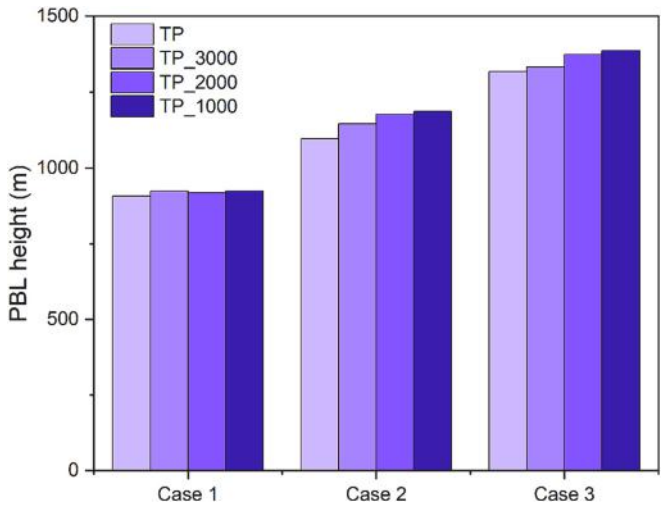

Fig. 4. Mean PBL height of the Tarim Basin with different Tibetan Plateau altitudes during the three dust cases: Case 1 (March 8–15), Case 2 (March 21–27), and Case 3 (April 10–18).

Fig. 5 shows the variation in the near-surface meteorological field of the Tarim Basin at different Tibetan Plateau altitudes during the three cases. Fig. 5a–c shows that Wind_10 was negatively correlated with the Tibetan Plateau altitude. The mean daily Wind_10 was 2.62 m/s, 3.02 m/s, and 2.75 m/s for Cases 1, 2, and 3, respectively. The daily Wind_10 increased by 0.92%, 5.65%, and 12.03% on average, when Tibetan Plateau altitudes decreased to 3000 m, 2000 m, and 1000 m, respectively. Although Wind_10 increased as the Tibetan Plateau altitude decreased, there were significant differences between these three cases. For example, as the Tibetan Plateau altitude decreased to 1000 m, the average Wind _10 increased by 15.57%, 9.31%, and 11.2% for Cases 1, 2, and 3, respectively. This may be related to the strength of the weather system during each dust process. The wind speed near the ground is an important parameter affecting dust emissions (Zhou et al., 2020). Our results indicated that an increase in Wind_10 could enhance dust emissions near the surface, which could rapidly increase the DC in the lower layers. However, an increase in the horizontal wind speed was not conducive to dust uptake to high altitudes.

SAT is another important thermal factor affecting sand saltation (Zhou et al., 2019), as shown for C_Exp and S_Exp in Fig. 5d–f. The mean daily SAT was 6.46 °C, 11.10 °C, and 18.19 °C for Cases 1, 2, and 3, respectively. In contrast to Wind_10, SAT remained nearly constant (a mean change of 0.07%) as the Tibetan Plateau altitude decreased to 3000 m. The daily SAT increased by 3.50% and 6.52% on average as the Tibetan Plateau altitudes decreased to 2000 m and 1000 m, respectively. The comparison results found that the impact of the Tibetan Plateau terrain on Wind_10 was significantly stronger than that on SAT. The saltation count in the TD was positively correlated with SAT as reported by Zhou et al. (2019) as the SAT was lower than 25 (±1) °C. The increase in SAT could lead to stronger evaporation rates, resulting in drier surfaces (Sankey et al., 2009; Barchyn and Hugenholtz, 2012). Therefore, an increase in SAT is favorable for dust emissions.

Atmospheric stability is a thermodynamic property that determines whether the atmosphere accelerates, suppresses, or does not affect the vertical movement of air masses. The atmosphere is unstable, with fully developing turbulence and convection and strong diffusion and dilution

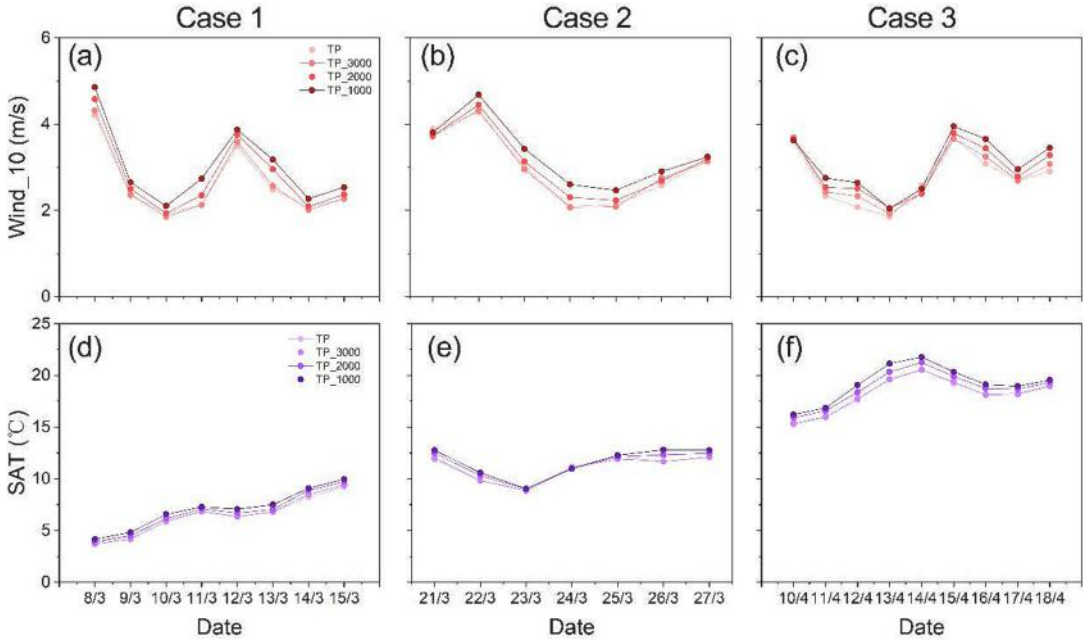

Fig. 5. Variation in Wind_10 and SAT at different Tibetan Plateau altitudes in the Tarim Basin on (a, d) March 8–15, (b, e) March 21–27, and (c, f) April 10–18.

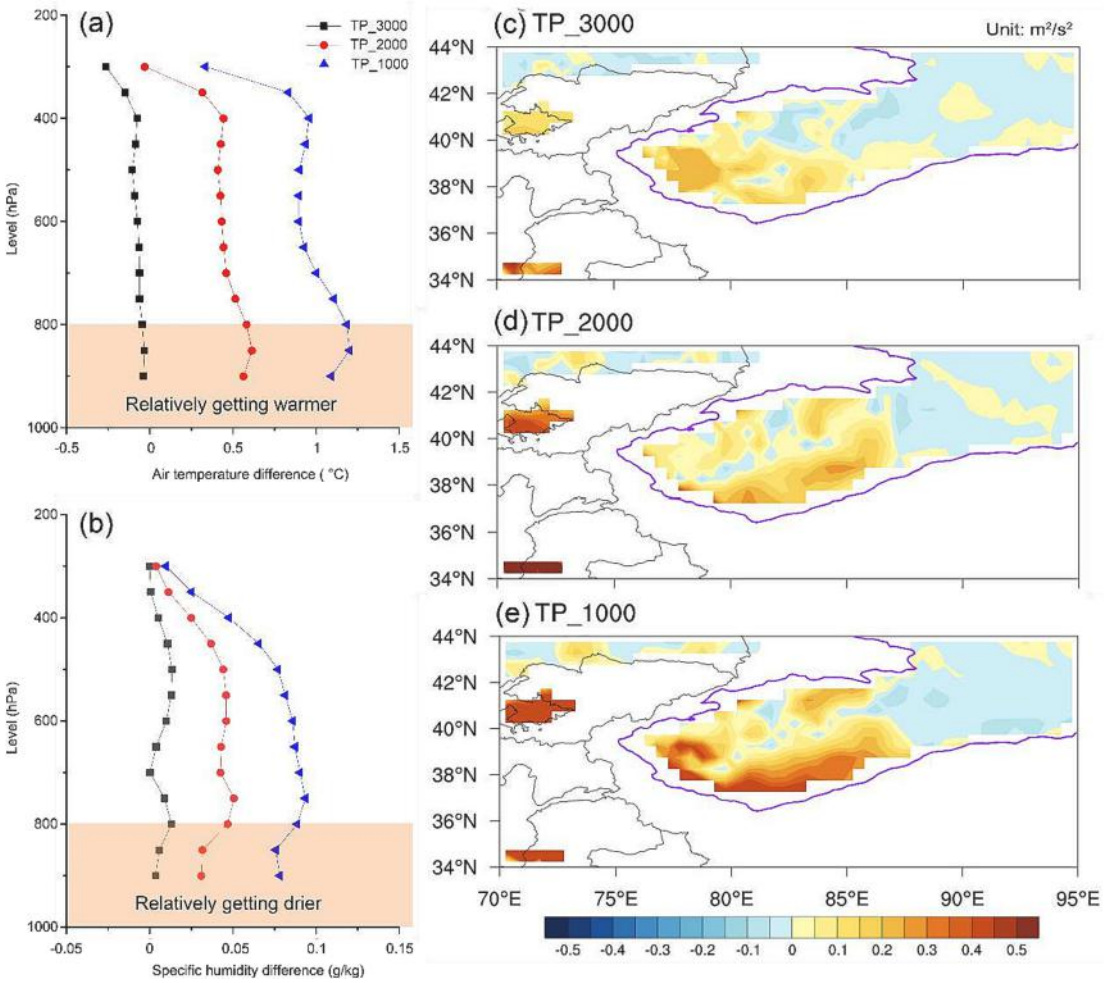

Fig. 6. Vertical distribution of mean air temperature (a) and specific humidity (b) difference between S_Exp and C_Exp during three dust cases. Spatial distribution of the mean convective available potential energy difference between S_Exp and C_Exp for the three dust cases (c, TP_3000; d, TP_2000; e, TP_1000).

capabilities. The vertical distribution of air temperature and specific humidity are the two important parameters for measuring atmospheric stability. Fig. 6a shows the vertical distributions of the mean air temperature differences between S_Exp and C_Exp for the three dust events. When the Tibetan Plateau altitude decreased to 3000 m, all atmospheric layers showed a weak cooling over the Tarim Basin, with an average decrease of approximately −0.09 °C. However, the air temperature showed a warming trend over the Tarim Basin as the altitude continued to decrease. The lower the Tibetan Plateau altitude, the more significant was the increase in the air temperature. The average air temperature increased by 0.43 °C and 0.94 °C as the Tibetan Plateau altitudes decreased to 2000 m and 1000 m, respectively. Fig. 6b shows the vertical distributions of the mean specific humidity differences between S_Exp and C_Exp for the three dust events. In contrast to the air temperature, all atmospheric layers showed wetting over the Tarim Basin, caused by the decrease in Tibetan Plateau altitude. The specific humidity increased by 0.01 g/kg, 0.04 g/kg, and 0.07 g/kg on average over the Tarim Basin as the Tibetan Plateau altitudes decreased to 3000 m, 2000 m, and 1000 m, respectively. Overall, as the barrier effect of the Tibetan Plateau disappeared, warm and humid air flowed from the south and entered the Tarim Basin, causing all atmospheric layers over the Tarim Basin to show warming and wetting trends. However, considering 800 hPa as the boundary, the amplitude of the increase in air temperature in the lower layers was greater than that in the upper layers, whereas an opposite trend was observed for the increase in specific humidity, as shown in the shadow. This implied that the decrease in the Tibetan Plateau altitude intensified the trend of warm drying in the lower layers and cold wetness in the upper layers over the Tarim Basin, and its atmospheric instability became more enhanced, which benefitted the upward transport of dust. Fig. 6c–e shows the mean convective available potential energy (CAPE) difference between S_Exp and C_Exp during the three dust events. The results indicated that atmospheric instability increased in the Tarim Basin, especially in the TD. Therefore, the results suggest that the decrease in the Tibetan Plateau altitude would enhance the vertical upward motion in the Tarim Basin.

To more accurately analyze the changes in the vertical distribution of dust aerosols over the Tarim Basin caused by the reduction in the Tibetan Plateau altitude, we further investigated the impact of the plateau terrain on the vertical circulation of the Tarim Basin. Fig. 7a shows the vertical cross section of the mean wind field along the Tarim Basin (81–84°E) for the three dust events, which suggested that weak updrafts occurred between 39°N and 40°N, whereas other areas of the Tarim Basin were dominated by downdrafts. As the Tibetan Plateau altitude decreased to 3000 m, the upward movement area began to shift towards the southern part of the Tarim Basin, forming a vertical circulation that rose to the south and sank to the north (Fig. 7b). As the Tibetan Plateau altitudes decreased continuously to 2000 m and 1000 m, vertical circulation was maintained, and its intensity continued to strengthen (Fig. 7c–d). Furthermore, as the Tibetan Plateau altitude decreased, the horizontal wind speed in the upper layers (Fig. 7b–d) improved. These results indicated that the Tibetan Plateau altitude decreased leads to the formation of local vertical circulation and influences the spatiotemporal distributions of dust aerosol over the Tarim Basin.

Fig. 3 shows that as the Tibetan Plateau altitude decreased, the DC increased in the lower layers and decreased in the upper layers over the Tarim Basin, with a boundary at 700 hPa. The enhancement of the horizontal wind speed in the upper layers accelerated the removal of suspended dust, which may be an important reason for the reduction in DC in the upper layers. However, there are multiple reasons for the DC increased in the lower layers. Enhancements in the PBL height, Wind_10, and SAT, but a weaking in the atmospheric stability, in the above analysis are important reasons for the DC increased in the lower layers.

In addition, Fig. 7e–g shows the vertical cross-section of the mean DC difference between S_Exp and C_Exp along the TD (81–84°E) for the three dust cases. The high-value center of the DC in the lower layers was located in the southern part of the TD, which was consistent with the changes in vertical circulation. Overall, the meteorological field and vertical circulation could explain the change in the three-dimensional structure of the dust in the Tarim Basin.

4. Discussion

The Tibetan Plateau is known as a “roof of the world” and a “third pole.” It plays an important role in the regional/global climate change and energy-water cycle (Zhu et al., 2021; Liu et al., 2020; Xu et al., 2008). The existence of the TP has changed the regional atmospheric circulation model in the Northern Hemisphere, resulting in the branching and circumfluence of the westerlies and the formation of north-south streams. The dynamic effect of the Tibetan Plateau is also manifested in its barrier effect on near-surface airflow, and the northern side of the TP is not easily affected by the warm and humid airflow from the south. Due to the influence of the deep Tarim Basin terrain, especially the Tibetan Plateau, coupled with the strong surface heating of the underlying desert and the vigorous convective and turbulent movements, the Tarim Basin experiences frequent dust events in spring and summer (Wang et al., 2019). Our results showed that with decreasing Tibetan Plateau altitude, both Wind_10 and SAT increased (Fig. 5), which in turn promoted dust emissions. Moreover, an increase in PBL height and atmospheric instability were also conducive to the vertical mixing of dust aerosol in the lower layers (Figs. 4 and 6). The formation of vertical circulation over the Tarim Basin (Fig. 7), especially the increase in the horizontal wind speed, led to low DC in the upper layers. Therefore, this study clearly indicates that the Tibetan Plateau terrain has a significant impact on the dust aerosol distribution over the Tarim Basin, as illustrated in Fig. 8. Of course, there may be some randomness when simulating individual cases, which need more simulation experiments to be verified. Furthermore, we are considering on analyzing how the dust aerosols are distributed over the Tarim Basin, as the Tarim Basin is landfilled and is as high as the Tibetan Plateau. The difference between these two areas will be investigated in our future studies.

5. Conclusions

The Tibetan Plateau significantly affects the dust aerosol distribution over the Tarim Basin, owing to the dynamic and thermal driving of its large terrain. Based on the WRF-Chem model, the impact of Tibetan Plateau terrain on the dust aerosol variations in three dust cases over the Tarim Basin was investigated in this study. The main conclusions are as follows.

As the Tibetan Plateau altitude decreased, characterization of DC by upper layers decreased and that by low layers increased over the Tarim Basin. Considering 700 hPa as the boundary line, the average DC increased by 13.72%, 31.39%, and 52.73% in the low layers; the average DC decreased by nearly 30% in the upper layers over the Tarim Basin as the Tibetan Plateau altitude dropped to 3000 m, 2000 m, and 1000 m, respectively. From the perspective of all atmospheric layers, the DC in the lower layers increasingly dominated the entire atmospheric layers with decreasing altitude. Therefore, the average DC of all atmospheric layers increased by 8.52%, 24.03%, and 43.05% in the Tarim Basin as the Tibetan Plateau altitudes dropped to 3000 m, 2000 m, and 1000 m, respectively.

Furthermore, the meteorological field in the Tarim Basin changed with the decrease in the Tibetan Plateau altitude, leading to enhanced PBL height, Wind_10, and SAT, but weakened atmospheric stability, all of which contributed to the increase in DC in the lower layers over the Tarim Basin. Additionally, the decrease in the Tibetan Plateau altitude formed a vertical circulation that rose in the south and sink in the north over the Tarim Basin, of which enhancing the horizontal wind speeds in the upper layers. Therefore, dust aerosols should not remain suspended for a long duration in the upper layers. Overall, meteorological field and vertical circulation could adequately explain the changes in the dust aerosol distribution over the Tarim Basin.

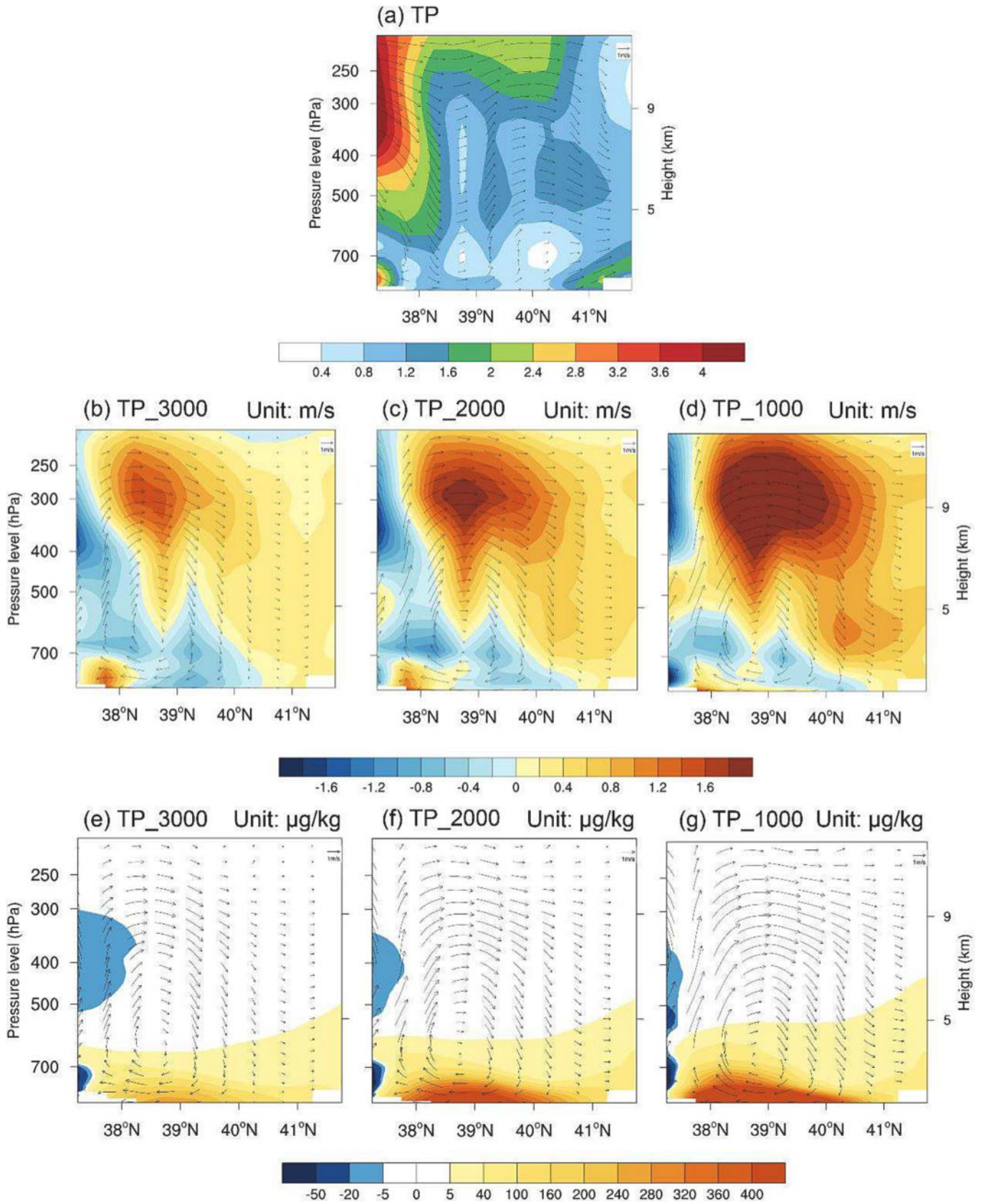

Fig. 7. Vertical cross-section of the mean wind field along the TD (81–84°E) during the three dust cases (a). Wind field (b, TP_3000, c, TP_2000, and d, TP_1000) and dust aerosol concentration (e, TP_3000, f, TP_2000, and g, TP_1000) difference between S_Exp and C_Exp. Colors represent the wind speed (b–d) and dust aerosol concentration (e–g), and the arrow represents the wind vector. The vertical velocity increased by 50 times.

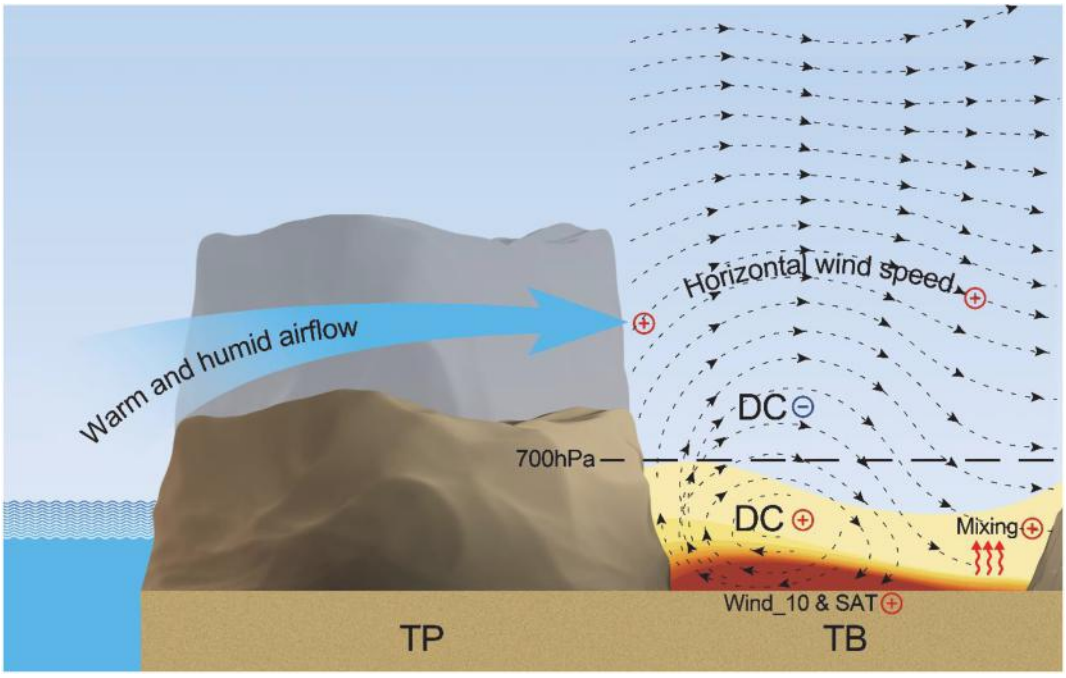

Fig. 8. Mechanism of the effect of the Tibetan Plateau terrain on dust aerosol distribution over the Tarim Basin. The gray area represents a decrease in the Tibetan Plateau altitude, blue arrow represents the warm and humid airflow, black arrows represent the vertical circulation, black dashed line represents the boundary of dust concentration change, and red arrows represent vertical mixing. The plus and minus signs indicate enhanced and weakened effects, respectively. TP and TB represent the Tibetan Plateau and Tarim Basin, respectively. (For interpretation of the references to colour in this figure legend, the reader is referred to the web version of this article.)

CRediT authorship contribution statement

Chenglong Zhou: Writing – original draft. **Xinghua Yang:** Conceptualization, Methodology. **Yuzhi Liu:** Conceptualization, Writing – review & editing. **Qingzhe Zhu:** Methodology. **Yongkun Xie:** Data curation. **Fan Yang:** Data curation. **Mamtimn Ali:** Data curation. **Wen Huo:** Data curation. **Qing He:** Data curation. **Lu Meng:** Data curation.

Declaration of Competing Interest

The authors declare no competing financial interests.

Data availability statement

The authors are grateful to the following science teams for providing the accessible data products used in this study. The MERRA-2 reanalysis data were provided by NASA Goddard Earth Science Data and Information Services Center through the NASA GES DISC online archive (https://goldsmr5.gesdisc.eosdis.nasa.gov/data). The meteorological observation data were supplied by the National Meteorological Information Center (http://data.cma.cn/) under license and so cannot be made freely available.

Acknowledgments

This research was supported by the Natural Science Foundation of Xinjiang Uygur Autonomous Region (2022D01A366) and jointly supported by the Strategic Priority Research Program of the Chinese Academy of Sciences (Grant No. XDA2006010301), Scientific and Technological Innovation Team (Tianshan Innovation Team) Project (Grant No. 2022TSYCTD0007), Fellowship of China postdoctoral Science Foundation (2022MD723851), National Natural Science Foundation of China (41875019, 41975010, 41905014), and the Fundamental Research Funds for the Central Universities (lzujbky-2020-kb02).

References

Barchyn, T.E., Hugenholtz, C.H., 2012. Winter variability of aeolian sediment transport threshold on a cold-climate dune. Geomorphology 177-178, 38–50. https://doi.org/10.1016/j.geomorph.2012.07.012.

Chamecki, M., Hout, R., Meneveau, C., Parlange, M., 2007. Concentration profiles of particles settling in the neutral and stratified atmospheric boundary layer. Bound.-Lay. Meteorol. 125, 25–38. https://doi.org/10.1007/s10546-007-9194-5.

Chen, S., Huang, J., Li, J., Jia, R., Jiang, N., Kang, L., Ma, X., Xie, T., 2017. Comparison of dust emissions, transport, and deposition between the Taklimakan Desert and Gobi Desert from 2007 to 2011. Sci. China. Earth. Sci. 60, 1338–1355. https://doi.org/10.1007/s11430-016-9051-0.

Chen, S., Tong, B., Dong, C., Liu, D., 2020. Retrievals of aerosol layer height during dust events over the Taklimakan and Gobi Desert. J. Quant. Spectrosc. Radiat. Transf. 254, 107198 https://doi.org/10.1016/j.jqsrt.2020.107198.

Fast, J., Gustafson, W., Easter, R., Zaveri, R., Barnard, J., Chapman, E., Grell, A., Peckham, E., 2006. Evolution of ozone, particulates, and aerosol direct radiative forcing in the vicinity of Houston using a fully coupled meteorology-chemistry aerosol model. J. Geophys. Res. Atmos. 111, D21305. https://doi.org/10.1029/2005JD006721.

Garratt, J.R., 1994. Review: the atmospheric boundary layer. Earth Sci. Rev. 37 (1–2), 89–134. https://doi.org/10.1016/0012-8252(94)90026-4.

Gelaro, R., Mccarty, W., Suárez, Max J., Todling, R., Molod, A., Takacs, L., Randles, C., Darmenov, A., Bosilovich, M.G., Reichle, R., Wargan, K., Coy, L., Cullather, R., Draper, C., Akella, S., Buchard, V., Conaty, A., da Silva, A., Gu, W., Kim, G.K., Koster, R., Lucchesi, R., Merkova, D., Nielsen, J.E., Partyka, G., Pawson, S., Putman, W., Rienecker, M., Schubert, S.D., Sienkiewicz, M., Zhao, B., 2017. The modern-era retrospective analysis for research and applications, version 2 (MERRA-2). J. Climate 30. https://doi.org/10.1175/JCLI-D-16-0758.1.

Ginoux, P., Chin, M., Tegen, I., Prospero, J., Holben, B., Dubovik, O., Lin, S., 2001. Sources and distributions of dust aerosols simulated with the GOCART model. J. Geophys. Res. 106, 20255–20274. https://doi.org/10.1029/2000JD000053.

Ginoux, P., Prospero, J.M., Torres, O., Chin, M., 2004. Long-term simulation of global dust distribution with the GOCART model: correlation with North Atlantic Oscillation. Environ. Model. Software 19, 113–128. https://doi.org/10.1016/S1364-8152(03)00114-2.

Grell, G., Peckham, S., Schmitz, R., Mckeen, S., Frost, G., Skamarock, W., Eder, B., 2005. Fully coupled "online" chemistry within the WRF model. Atmos. Environ. 39, 6957–6975. https://doi.org/10.1016/j.atmosenv.2005.04.027.

Hoffmann, C., Funk, R., 2015. Diurnal changes of PM_{10} emission from arable soils in NE-Germany. Aeolian Res. 17, 117–127. https://doi.org/10.1016/j.aeolia.2015.03.002.

Huang, J., Fu, Q., Su, J., Tang, Q., Minnis, P., Hu, Y., Yi, Y., Zhao, Q., 2009. Taklimakan dust aerosol radiative heating derived from CALIPSO observations using the Fu-Liou radiation model with CERES constraints. Atmos. Chem. Phys. 9, 4011–4021. https://doi.org/10.5194/acp-9-4011-2009.

Huang, J., Wang, T., Wang, W., Li, Z., Yan, H., 2014. Climate effects of dust aerosols over East Asian arid and semiarid regions. J. Geophys. Res. Atmos. 119 https://doi.org/10.1002/2014JD021796.

Huneeus, N., Schulz, M., Balkanski, Y., Griesfeller, J., Prospero, J., Kinne, S., Bauer, S., Boucher, O., Chin, M., Dentener, F., Diehl, T., Easter, R., Fillmore, D., Ghan, S., Ginoux, P., Grini, A., Horowitz, L., Koch, D., Krol, M.C., Landing, W., Liu, X., Mahowald, N., Miller, R., Morcrette, J.J., Myhre, G., Penner, J., Perlwitz, J., Stier, P., Takemura, T., Zender, C.S., 2011. Global dust model intercomparison in AeroCom phase I. Atmos. Chem. Phys. 11, 7781–7816. https://doi.org/10.5194/acp-11-7781-2011.

Jia, R., Liu, Y., Hua, S., Zhu, Q., Shao, T., 2018. Estimation of the aerosol radiative effect over the Tibetan Plateau based on the latest CALIPSO product. J. Meteorol. Res. 32, 707–722.

Li, Q., Wu, B., Liu, J., Zhang, H., Cai, X., Song, Y., 2020. Characteristics of the atmospheric boundary layer and its relation with $PM_{2.5}$ during haze episodes in winter in the North China Plain. Atmos. Environ. 223, 117265 https://doi.org/10.1016/j.atmosenv.2020.117265.

Li, Q., Zhang, H., Cai, X., Song, Y., Zhu, T., 2021. The impacts of the atmospheric boundary layer on regional haze in North China. Npj. Clim. Atmos, Sci. 4 (1), 1–10. https://doi.org/10.1038/s41612-021-00165-y.

Liu, Y., Huang, J., Shi, G., Takamura, T., Khatri, P., Bi, J., Shi, J., Wang, T., Wang, X., Zhang, B., 2011. Aerosol optical properties and radiative effect determined from sky-radiometer over Loess Plateau of Northwest China. Atmos. Chem. Phys. 11 (22) https://doi.org/10.5194/acp-11-11455-2011, 11455e11463.

Liu, Y., Shi, G., Xie, Y., 2013. Impact of dust aerosol on glacial-interglacial climate. Adv. Atmos. Sci. 30 (6), 1725e1731. https://doi.org/10.1007/s00376-013-2289-7.

Liu, Y., Rui, J., Dai, T., Xie, Y., Shi, G., 2014. A review of aerosol optical properties and radiative effects. J. Meteorol. Res. 8, 1003–1028. https://doi.org/10.1007/s13351-014-4045-z.

Liu, L., Huang, X., Ding, A., Fu, C., 2016a. Dust-induced radiative feedbacks in North China: a dust storm episode modeling study using WRF-Chem. Atmos. Environ. 129, 43–54. https://doi.org/10.1016/j.atmosenv.2016.01.019.

Liu, C., Zhao, T., Yang, X., Liu, F., Han, Y., Luan, Z., He, Q., Rood, M., Yuen, W., 2016b. Observational study of formation mechanism, vertical structure, and dust emission of dust devils over the Taklimakan Desert. China. J. Geophys. Res. Atmos. 121 (7), 3608–3618. https://doi.org/10.1002/2015JD024256.

Liu, Y., Li, Y., Huang, J., Zhu, Q., Wang, S., 2020. Attribution of the Tibetan Plateau to northern drought. Natl. Sci. Rev. 7 (3), 489–492. https://doi.org/10.1093/nsr/nwz191.

Luo, R., Liu, Y., Zhu, Q., Luo, M., Tan, Z., Shao, T., 2022. Anthropogenic pollutants could enhance aridity in the vicinity of the Taklimakan Desert: a case study. Sci. Total Environ. 838 (4), 156574 https://doi.org/10.1002/joc.7089.

Mahowald, N.M., 2011. Aerosol indirect effect on biogeochemical cycles and climate. Science 334, 794–796.

Meng, L., Zhao, T., He, Q., Yang, X., Mamtimin, Ali, Yang, Fan, Zhou, C., Huo, W., Wang, M., Pan, H., Yang, J., 2022. Climatic characteristics of floating dust and persistent floating dust over the Tarim Basin in the recent 30 years. Acta. Meteor. Sin. 80 (2), 322–333. https://doi.org/10.11676/qxxb2022.022. (In Chinese).

Molod, A., Takacs, L., Suarez, M., Bacmeister, J., 2015. Development of the GEOS-5 atmospheric general circulation model: evolution from MERRA to MERRA2. Geosci. Model Dev. 8, 1339–1356. https://doi.org/10.5194/gmd-8-1339-2015.

Pan, Y., Chamecki, M., Isard, S., 2013. Dispersion of heavy particles emitted from area sources in the unstable atmospheric boundary layer. Bound.-Lay. Meteorol. 146, 235–256. https://doi.org/10.1007/s10546-012-9753-2.

Prospero, J.M., Collard, F.X., Molinié, J., Jeannot, A., 2014. Characterizing the annual cycle of African dust transport to the Caribbean Basin and South America and its impact on the environment and air quality. Global. Biogeochem. Cy 18, 400–414. https://doi.org/10.1002/2013GB004802.

Sakaeda, N., Wood, R., Rasch, P.J., 2011. Direct and semidirect aerosol effects of southern African biomass burning aerosol. J. Geophys. Res. Atmos. 116 (D12), D12205. https://doi.org/10.1029/2010jd015540.

Sankey, J.B., Germino, M.J., Glenn, N.F., 2009. Relationships of post-fire aeolian transport to soil and atmospheric conditions. Aeolian Res. 1 (1–2), 75–85. https://doi.org/10.1016/j.aeolia.2009.07.002.

Shao, T., Liu, Y., Wang, R., Zhu, Q., Tan, Z., Luo, R., 2022. Role of anthropogenic aerosols in affecting different-grade precipitation over eastern China: a case study. Sci. Total Environ. 807, 150886 https://doi.org/10.1016/j.scitotenv.2021.150886.

Wang, S., Wang, J., Zhou, Z., Shang, K., Yang, D., Zhao, Z., 2003. Regional characteristics of dust events in China. J. Geogr. Sci. 58 (2), 193–200. https://doi.org/10.1007/BF02873145.

Wang, M., Xu, X., Xu, H., Lenschow, D.H., Zhou, M., Zhang, J., Wang, Y., 2019. Features of the deep atmospheric boundary layer over the Taklimakan Desert in the summertime and its influence on regional circulation. J. Geophys. Res. Atmos. 124 (23), 12755–12772. https://doi.org/10.1029/2019JD030714.

Xu, X., Zhang, R., Koike, T., Lu, C., Shi, X., Zhang, S., Bian, L., Cheng, X., Li, P., Ding, G., 2008. A new integrated observational system over the Tibetan plateau. B. AM. Meteorol. Soc. 89 (10), 1492–1496. https://doi.org/10.1175/2008BAMS2557.1.

Yang, X., Shen, S., Yang, F., He, Q., Mamtimin, A., Huo, W., Liu, X., 2016. Spatial and temporal variations of blowing dust events in the Taklimakan Desert. Theor. Appl. Climatol. 125 (3–4), 669–677. https://doi.org/10.1007/s00704-015-1537-4.

Zhang, H., Li, X., 2014. Review of the field measurements and parameterization for dust emission during sand-dust events. J. Meteorol. Res. 28, 903–922. https://doi.org/10.1007/s13351-014-3296-z.

Zhang, D., Liu, D., Luo, T., Wang, Z., Yin, Y., 2015. Aerosol impacts on cloud thermodynamic phase change over East Asia observed with CALIPSO and CloudSat measurements. J. Geophys. Res. Atmos. 120, 1490e1501. https://doi.org/10.1002/2014JD022630.

Zhou, C., Mamtimin, A., Pan, H., Yang, F., Yang, X., 2019. Relationship between air temperature and horizontal sand-dust flux observed in the taklimakan desert, China. Theor. Appl. Climatol. 138 (3–4), 1845–1852. https://doi.org/10.1007/s00704-019-02946-1.

Zhou, C., Yang, F., Mamtimin, A., Huo, W., Liu, X., He, Q., Yang, X., 2020. Wind erosion events at different wind speed levels in the Tarim Basin. Geomorphology 369 (1), 107386. https://doi.org/10.1016/j.geomorph.2020.107386.

Zhou, C., Liu, Y., Zhu, Q., He, Q., Zhao, T., Yang, F., Huo, W., Yang, X., Mamtimin, A., 2022a. In situ observation of warm atmospheric layer and the heat contribution of suspended dust over the Tarim Basin. Atmos. Chem. Phys. 22, 5195–5207. https://doi.org/10.5194/acp-22-5195-2022.

Zhou, C., Liu, Y., He, Q., Zhong, X., Zhu, Q., Yang, F., Huo, W., Mamtimin, A., Yang, X., Wang, Y., Meng, L., 2022b. Dust characteristics observed by unmanned aerial vehicle over the Taklimakan Desert. Remote Sens. (Basel) 14, 990. https://doi.org/10.3390/rs14040990.

Zhu, Q., Liu, Y., Shao, T., Luo, R., Tan, Z., 2021. Role of the Tibetan Plateau in northern drought induced by changes in the subtropical westerly jet. J. Climate 12, 34. https://doi.org/10.1175/JCLI-D-20-0799.1.